ORIGINAL RESEARCH ARTICLE

HIsarna Process Simulation Model: Using FactSage with Macro Facility

ZHIMING YAN, THEINT THEINT HTET, JOHANNES HAGE, KOEN MEIJER, and ZUSHU LI

The HIsarna process is one of the emerging technologies for reducing the carbon footprint of the ironmaking process, which is currently in the pilot plant stage. A kinetic HIsarna process simulation model based on the effective equilibrium reaction zone concept has been developed using the FactSage macro programming facility to advance understanding of the whole process. In the model, the HIsarna process is conceptually divided into various equilibrium zones involving combustion, coal pyrolysis and gasification, gas/slag/carbon reactions, and slag/metal reaction. The model has been validated through the pilot plant data, and the results are in good agreement with the quantity and composition of hot metal, slag, and gas. The HIsarna off-gas stream with high CO_2 content can potentially allow capture and storage directly for carbon mitigation. The utilization of titanium magnetite ore in the HIsarna process has also been investigated *via* the developed model. The injection of titanium magnetite ore which has high FeO content decreases coal consumption. Still, it increases the slag volume as higher gangue content when keeping the same productivity as the pilot plant trial. The HIsarna process shows promising potential in using low-quality high titania iron ore as feed materials, but the slag system needs to be further optimized. From the heat distribution, the off-gas sensible heat accounts for a large part of the input heat due to its high temperature but can be recovered with good efficiency. The present model is an efficient tool for understanding the HIsarna process and providing theoretical guidance for future pilot research.

https://doi.org/10.1007/s11663-023-02732-5

I. INTRODUCTION

THE steel industry is one of the industries with the highest CO_2 emission due to using fossil fuels as primary reductant and heating agents for iron and steel production. On average, 1.80 tons of CO_2 were emitted for every ton of steel produced in 2020. The steel industry generates more than 3000 megatons of direct emissions, approximately nine percent of the global use of fossil fuels.[1] To mitigate the increasing CO_2 emission from the steel industry, several alternative ironmaking technologies for energy-efficiency improvement and carbon dioxide emissions reduction have been proposed by researchers worldwide. In Europe, ULCOS (Ultra Low CO_2 Steelmaking) program was established in 2004 to develop technologies to reduce CO_2 emissions by at least 50 pct before 2050 compared to the 1990 level. HIsarna is one of the innovative ironmaking technologies under the ULCOS developed by Tata Steel Europe. Recent HIsarna pilot-scale trials successfully demonstrated 50 pct CO_2 emissions reduction without Carbon Capture and Storage (CCS), and 80 pct CO_2 emissions reduction can be achievable with CCS.[2] Other attractions of the HIsarna process include the ability to use low-quality iron ore (*e.g.*, TiO_2-containing magnetite, high-Al_2O_3/P/Zn iron ore), using diversified fuels from thermal coals, gas fuels, to biomass instead of coking coals, and ease to capture a high proportion of CO_2.[3,4]

HIsarna process involves two main technologies of Cyclone Converter Furnace (CCF) and HIsmelt Smelt Reduction Vessel (SRV). Iron ore and fluxes are injected into the CCF, together with oxygen. Hot gas with a certain CO content from the SRV is post-combusted in the CCF, increasing the temperature and enabling the iron ore to melt and be partially pre-reduced. The molten and partially reduced iron ore forms a liquid film along the cyclone wall and drops down into the slag layer in the SRV. Fuel (carbonaceous material) is injected into the slag layer, which will reduce the FeO in the iron-bearing

ZHIMING YAN, THEINT THEINT HTET, and ZUSHU LI are with the WMG, University of Warwick, Coventry, CV4 7AL, United Kingdom. Contact e-mail: Zhiming.Yan@warwick.ac.uk; Z.Li.19@warwick.ac.uk JOHANNES HAGE and KOEN MEIJER are with the IJmuiden Technology Centre, PO Box 10000, 1970 CA IJmuiden, The Netherlands.

Manuscript submitted June 11, 2022; accepted January 17, 2023.
Article published online February 15, 2023.

slag and carburize the hot metal. The CO gas from reduction and gasification reactions will be partly combusted with injected oxygen in the space on the top of slag for generating heat. The splash and turbulence resulting from the injection processes ensure part of this heat is transported to the slag and metal bath.

The HIsarna pilot plant established in *IJmuiden, the Netherlands*, with a nominal capacity of 60,000 tons/year, has been conducting several trial campaigns in the last few years. To better understand the process for optimizing the operation and up-scaling, developing a kinetic simulation model for the HIsarna process is necessary. For an accurate kinetic simulation of a process involving solid, gas, slag and hot metal, the diffusivities of all species and the thermodynamic descriptions of all phases are needed. However, this kind of accurate model is challenging to perform in practice due to the computational difficulty and lack of diffusivity data. Recently, the combination of the thermodynamic database (such as FactSage, CEQCSI) and the equilibrium reaction zone model (EERZ) provides another possibility, which has been used by other researchers for modeling various metallurgical processes.[5–13] Srivastava *et al.*[5] developed a model for COREX Melter gasifier and was further developed by Kadrolkar *et al.*[6] to precisely predict the reducing gas compositions and determine the process exergy losses. Srishilan *et al.*[7] also developed a model to predict the compositions and quantities of the hot metal, slag, and reducing gas generated for different degrees of metallization of the COREX process. Kumar *et al.*[8] used FactSage to estimate CO_2 emissions from rotary hearth furnaces using different reductant coals and external fuel gases to produce sponge iron. In the steel secondary refining process, Ende *et al.*[9–11] developed kinetic models to simulate the decarburization reaction in the Ruhrstahl Heraeus (RH) degassing process and the slag/metal interactions in the ladle furnace (LF) process, and the interactions between the mold flux/steel by using the FactSage macro processing. The rotary cement kiln process has been modeled by Thompson *et al.*[12] for tracing the alkali mobilization, in which thermodynamic equilibrium calculations are linked *via* the FactSage macro facility to a spreadsheet representation of zones in the kiln. Recently, Moosavi-Khoonsari *et al.*[13] developed a kinetic model for hot model pretreatment with powder injection based on the EERZ approach in combination with FactSage thermodynamic databases, providing a powerful tool for further optimization of the existing hot metal pretreatment process.

In this work, a kinetic model for the HIsarna process is developed by coupling the dynamics of the process with the thermodynamic database based on the EERZ concept. The accuracy of the model is demonstrated with pilot plant data. Titanium-containing magnetite ore as the feed material is investigated using the developed model to provide guidance for future pilot trials.

II. MODELING

A. *Concept of the HIsarna Process Model*

The effective equilibrium reaction zone model (EERZ) has been already demonstrated for steelmaking process units.[9–14] In the EERZ model, a complex process is divided into a finite number of reaction zones in which all phases within the "effective reaction zone" located near the reaction interface are assumed to reach equilibrium. With this assumption, the kinetics of reactions are taken into account by varying the reaction zone volumes. Effective reaction volumes are used instead of the mass transfer effect depending on the process conditions. The mass transfer coefficients or directly effective reaction zone volumes can be described by simulation results, experimental studies, and plant data. On this hand, the method can easily build a bridge between the thermodynamic database and the kinetic simulation. All reaction heats and heat losses are considered and tracked during the simulation, either isothermal or adiabatic. The combustion reactions are the main source of heat in the HIsarna process. There are many possibilities of heat consumption, for example, (i) the coal pyrolysis and gasification phenomena, (ii) the melting of iron ore/flux, (iii) the reduction reactions, (iv) the sensible heat of hot metal, slag, off-gas, and (v) the heat losses.

The proposed simulation of the HIsarna process considers twelve equilibrium reaction zones, as shown in Figure 1. In the schematic diagram, each reaction zone represents the following:

R1: Combustion in CCF, $\Delta H_{R1} = 0$;
R2: Melting and pre-reduction of iron ore, T = 1500 °C, ΔH_{R2};
R3: CCF off-gas homogenisation, ΔH_{R3};
R4: Molten ore gas reduction, T = 1500 °C, ΔH_{R4};
R5: Mixture of molten ore in slag layer, T = 1450 °C, ΔH_{R5};
R6: Coal pyrolysis and gasification, T = 1450 °C, ΔH_{R6};
R7: Slag reduction, T = 1450 °C, ΔH_{R7};
R8: Slag/hot metal reaction, T = 1450 °C, ΔH_{R8};
R9: Combustion in SRV, $\Delta H_{R9} = 0$;
R10: SRV off-gas homogenisation, T = 1450 °C, ΔH_{R10};
R11: Slag homogenisation, T = 1450 °C, ΔH_{R11};
R12: Hot metal homogenisation, T = 1450 °C, ΔH_{R12};

B. *Key Reaction Zones and Main Assumptions*

1. *Reaction zones in CCF*

In CCF, the hot gas from SRV mixes with the injected oxygen, and adiabatic combustion occurs in the reaction zone R1. In order to measure the energy utilization efficiency of the HIsarna furnace, Post Combustion Ratio (PCR) is introduced and defined as follows,

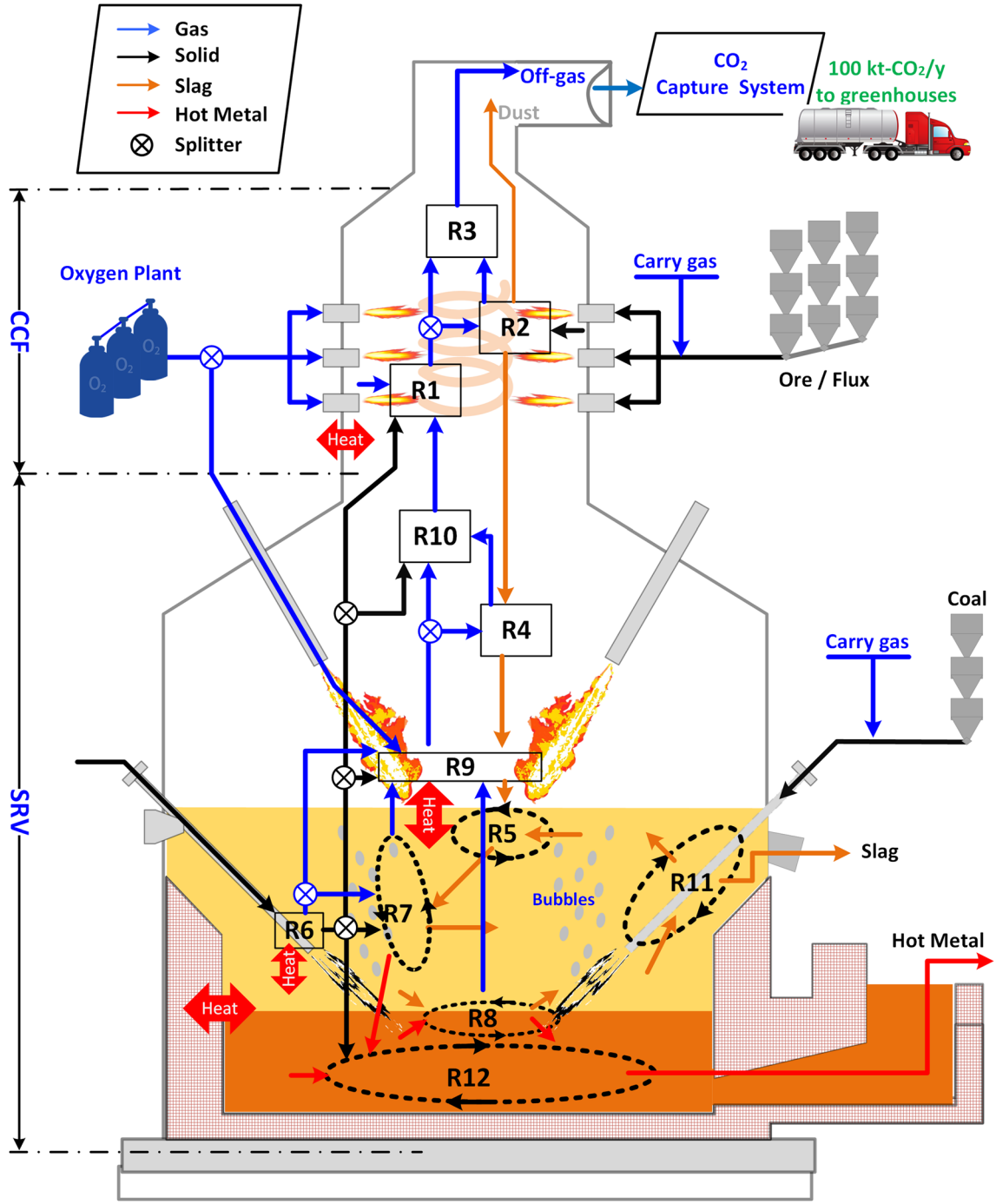

Fig. 1—Schematic diagram of reaction zones of the present HIsarna furnace model.

$$PCR = \frac{(volpct\mathrm{CO_2} + volpct\mathrm{H_2O})}{(volpct\mathrm{CO} + volpct\mathrm{CO_2} + volpct\mathrm{H_2} + volpct\mathrm{H_2O})} \times 100 \text{ pct} \quad [1]$$

The higher the PCR means, the higher the energy utilization. A PCR of 100 pct indicates that the carbon and hydrogen in the furnace are fully utilized and oxidized to CO_2 and H_2O. Of course, the purpose is to use the energy from fuel as much as possible to melt and reduce the injected iron ores. Therefore, partly gas stream from the reactor R1 with high temperature is reacted adiabatically with the injected iron ore and flux (air as the carrier gas, and the oxygen from air will react with the gas from R1 to generate heat) in reaction zone R2, enabling the iron ore and flux to melt and be partially pre-reduced. The molten ore which drops into SRV in the process could be determined *via* CCF capture efficiency, typically 90 pct or better, and the rest part is considered as dust loss. Assuming all the iron ore and flux are melted, the gas volume from R1 could be

determined by using the temperature of molten ore from pilot plant data. The remaining part of R1 gas is equilibrated with R2 gas in reactor R3, and the heat loss of CCF is considered *via* the ΔH_{R3} in the calculation.

2. *Reaction zones R4 and R5*

The molten and partly pre-reduced iron ore would be further reduced by the gas during the falling process in reactor R4, then passes through the combustion reactor in SRV (R9, adiabatic combustion) and drops into the slag layer (R5). According to the pilot plant trials, it can be assumed that the initial volume of slag in the hearth is 25 tons. During the calculation, the time step is 60 s (Δt = 60 s) and 1 h calculation for the process with plant data. Then the iron ore is replaced by titanium magnetite ore for 24 h duration calculation. Slag accumulates due to the sum of gangue, bottom ash, and flux. The slag is tapped every 3 h and keep 25 tons during tapping. Because of the strong motion of the slag caused by the coal injection and jet of oxygen lance, the molten ore drops from the CCF and the inventory slag are supposed to mix rapidly.

3. *Reaction zone of coal pyrolysis*

Reactor R6 deals with the coal pyrolysis and gasification phenomena. The coal is injected directly into the slag near the metal interface, and therefore, the reaction temperature can be considered the same as slag. After isothermal calculation, solid carbon, gas, and melted ash are generated, which are saved as streams for subsequent reactions, and the ΔH_{R6} reflects the heat consumption for coal pyrolysis and gasification.

4. *Reaction zones of reduction*

There is a reaction at the slag/metal interface, and the first-order mass transfer equation of species in one solution can be expressed as below:[10]

$$J_i = k_i\left(pctC_{i,bulk} - pctC_{i,interface}\right), \quad [2]$$

where J_i is the flux of i, k_i is the mass transfer coefficient of i, $pctC_{i,\ bulk}$ is the concentration of i species at bulk, and $pctC_{i,\ interface}$ is the concentration of i species at interface. Assuming the k_i of all species have the same values, then the amount of each solution reacted at the interface can be simply derived as follows:[8]

$$W_{solution} = (k\rho A)_{solution}\Delta t, \quad [3]$$

where W, k, and ρ are the reacting amount, overall mass transfer coefficient, and density of the given solution, respectively; A is the area of reaction interface, and Δt is the time step of the reaction. Because of the strong stirring of slag in the SRV vessel, the slag-metal mass transfer coefficient used here from the literature involves a strongly gas-stirred ladle.[14] Due to the stirring effect, it is difficult to determine the reaction area of the slag-metal reaction. Considering that the stirring is mainly concentrated in the slag, to simplify the model, it is assuming that the reaction interface area of the slag-metal reaction (R8) is the top surface area of the molten iron, which can be determined from the dimension of SRV hearth. In this case, the hot metal produced from R8 can be obtained. According to the yield of hot metal from the pilot plant tests, the carbon used for direct reduction can be determined in R7. All the gas from coal pyrolysis is assumed to react with slag before combustion. The volume of slag reacting with carbon and gas is estimated to be 10 pct of the inventory slag. Increasing the slag volume does not significantly affect the amount of hot metal produced during the reduction process due to the solid carbon diffusion control.

5. *Reaction zones of combustion and homogenization in SRV*

The heat needed for coal pyrolysis and reduction is supplied by combustion reaction R9. Gas streams from the reactors R7, R8 and unreacted carbon from R6 have combusted adiabatically with injected oxygen to generate the required heat in reactor R9. The SRV off-gas homogenization and slag homogenization are considered in reactors R10 and R11, respectively. The metal from reduction reactions (R7 and R8) is carbonized by the carbon from R6 and homogenized with inventory hot metal in reactor R12. The inventory of hot metal in the hearth always keeps being 42 tones, which means a steady hot metal tapping exits during a stable operating period. The complete homogenization of chemistry and temperature of the gas (R10), slag (R11), and hot metal (R12) are assumed despite of possible dead zone existence.

6. *Reaction zones of refractory dissolution*

Refractory can dissolve into the slag, as well as the hot metal. The dissolution rate can be affected by many factors, such as the physical and chemical conditions of the refractory and molten slag, the wetting ability between slag and refractory, as well as the physical erosion of fluids. However, refractory dissolution is not taken into account in the HIsarna kinetic model as it has a minor effect on the process.

7. *Heat balance*

During the HIsarna pilot plant trials, the temperature in the furnace was measured and recorded. The temperatures in different reaction zones are controlled to be relatively stable for steady operation. Also, the heat loss is not clear. Therefore, when constructing the model, all reactions except combustion reactions are set as isothermal reactions according to the data obtained from pilot plant trials. The relatively stable temperature in the SRV is mainly provided by the combustion reaction in the SRV upper space through diffusion and radiation, in addition to the heat from the reaction itself. The heat generated /consumed in each reaction zone is reflected by the reaction enthalpy change (ΔH_i) in the calculation process. By treating the entire HIsarna process in a certain period as an isolated system, the sum of the enthalpy changes of all reaction zones and heat loss should be zero, then

$$H_{heatloss} + \sum \Delta H_{Ri} = 0, \quad [4]$$

where ΔH_{Ri} is the reaction enthalpy change of reaction *Ri*. The sensible heat of hot metal, slag, off-gas, and dust can be calculated from the enthalpy change of materials stream from high temperature to room temperature (20 °C). The heat load is calculated based on the calorific value of the coal.

C. *Thermodynamic Database and Calculation Procedure*

FactSage is a powerful tool for thermodynamic modeling with the most well-known databases in the iron and steelmaking processes.[15] The parameters for multicomponent slag using the modified quasi-chemical (MQM) model in the FToxid database are critically optimized and self-consistent, and the random mixing model and new optimizations with the MQM are be combined to give a more accurate description of the liquid steel phase, and gas phase is an ideal solution. In the FactSage software, the kinetic process simulation models can be made by connecting FactSage databases and mass transport phenomena using Macro Processing Facility. The input data/conditions and output results can be stored in a simple text file or Microsoft Excel worksheets and transferred to the following related equilibrium calculations using this macro processing code. The FactSage software (version 7.3, ThermFact/CRCT, Montreal, Canada, and GTT-Technologies, Aachen, Germany) is used for all above reaction zones' calculation one by one in the order of reactions number. The *FactPS, FToxid, and FTmisc* databases are chosen to perform the calculations. All the stoichiometric solid and liquid compounds and solution databases are evaluated/optimized by the FACT group,[16] which are suitable for calculations involving ironmaking and steelmaking processes. The overall calculation flow chart of the proposed model is shown in Figure 2. The macro-based program calculates all the reaction zones one by one in the order of reaction numbers at each time step ($\Delta t = 60$ s) to ensure the successive calculation and loop computation feasibility for the iterative values of different reaction zones. In this way, the heat and the chemistry route of each reaction zone can be recorded simultaneously.

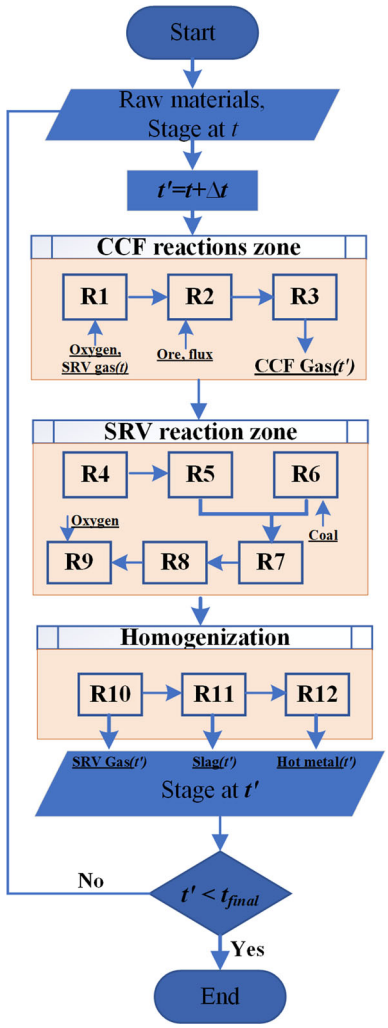

Fig. 2—The overall calculation flow chart of the HIsarna process model.

III. RESULTS AND DISCUSSION

A. *Model Validation*

The present model is applied to simulate the HIsarna pilot plant trial. The inputs to the model are from plant trial data, and the outputs are calculated from the developed model, which are summarized in Table I. The compositions of the main input raw materials are shown in Table II. Hot metal production was around 7 tons per hour (t/h) with a coal consumption of nearly 730 kg per ton of hot metal (kg/tHM), and the slag generation rate was 277 kg/tHM, which are in good agreement with those from pilot plant trials data.

The comparison of slag composition and hot metal composition between the calculated and the pilot plant data is shown in Figure 3. The composition of hot metal and slag produced by the HIsarna process is slightly different from that of a typical blast furnace (BF) iron making process. Due to the presence of coke in the BF hearth, the carbon in BF hot metal is saturated. There is

Table I. The Input and Output of the Model Calculation

Items	Amount	Unit	Items	Amount	Unit
Iron Ore Fines	11.85	t/h	hot metal	6.99	t/h
Flux Lime	0.55	t/h	slag	1.92	t/h
Coal	5.09	t/h	SRV gas	9.66	kNm^3/h
Carrier Gas—Air	1.16	kNm^3/h	CCF gas	12.03	kNm^3/h
Carrier Gas—N_2	0.69	kNm^3/h	dust	0.77	t/h
CCF Oxygen	2.55	kNm^3/h			
SRV Oxygen	3.80	kNm^3/h			

a discrepancy between the model and pilot plant values for S and P. The possible reason is that the model assumes the mass transfer coefficient of all species has the same values. The oxygen potential in the BF hearth is lower than that in SRV, resulting in almost no FeO maintaining in the BF final slag, which is good for desulfurization. On the contrary, the HIsarna slag has a higher oxygen potential of about 7 wt pct FeO, which is hard to reduce silica and manganese, as well as a weak desulfurization ability. The phase diagram of CaO-SiO_2-FeO-6wt pct MgO-14wt pct Al_2O_3-4wt pct MnO calculated from FactSage is shown in Figure 4. The red point indicates the slag composition of the pilot plant trial. The slag basicity (CaO wt pct/SiO_2 wt pct) is around 1.25, the liquids temperature of slag is slightly higher than 1350 °C, and the first precipitation phase is Melilite during the cooling process. The temperature of the SRV hearth zone fluctuates around 1450 °C, which is similar to the temperature of the BF hearth. To improve the desulfurization ability of slag, increasing the basicity is an effective way. However, for the current slag system, due to the small gap between the isothermal liquidus lines (Figure 4), increasing the basicity will cause the liquidus temperature to rise sharply. Increasing the FeO in a certain content results in the lower liquids temperature of slag, while the metal yield would decrease as expected. HIsarna process has an excellent ability to remove phosphorous from hot metal. Around 90 pct of the phosphorous is removed to slag, and this is a direct result that relates to the oxidizing condition.[17] Phosphorous tolerance has become a major issue due to the exhaustion of high-quality ore in some parts of the world, while the HIsarna process could be a promising technology to deal with high phosphorus iron ore.

The comparison of the calculated compositions of SRV gas and CCF gas with pilot plant data is shown in Figure 5. The modeling results are in good agreement with those from pilot plant trials in terms of compositions and gas volume. The gas from SRV with a certain amount of CO will be fully combusted in CCF to generate heat for the iron ore melting and iron ore pre-reduction. During this pilot plant campaign, the high PCR measured (more than 95 pct) in CCF demonstrates high energy efficiency with little scope for further heat released by combustion of the process gases. There is about 15 vol pct of N_2 remaining in the CCF off-gas due to the use of air as the carrier gas for iron ore and N_2 gas as the carrier gas for thermal coal. This off-gas stream with high enough CO_2 content can potentially allow direct capture and storage for carbon mitigation. No need for CO_2 scrubber offers significant advantages in terms of capital cost and energy efficiency.

Table II. Composition of Input Materials (Wt Pct)

	Iron ore	Lime	Coal Composition			
Fe_2O_3	89.68	0.44	Volatiles	7.20	ash	
FeO	0.93	/	Fixed C	86.20	Na_2O	0.76
Al_2O_3	1.37	0.23	Ash	6.70	MgO	1.44
SiO_2	4.20	0.50	Moisture	2.19	Al_2O_3	30.11
CaO	1.27	95.09	ultimate analy-		SiO_2	46.69
MgO	0.44	1.53	sis:		P_2O_5	1.74
MnO	0.38	/	C	86.4	K_2O	2.66
TiO_2	0.63	/	H	3.18	CaO	3.56
P_2O_5	0.06	/	O	1.16	TiO_2	1.82
S	0.0045	0.092	N	1.70	MnO	0.11
Moisture	0.10	/	S	0.88	Fe_2O_3	10.89
LOI	0.92	2.11	Ash	6.70	V_2O_5	0.17
Total	100	100	Total	100	Total	100

B. *Utilization of Titanium Magnetite Ore*

Titanium magnetite is a mineral containing oxides of titanium and iron, which is used as the raw material for smelting ferrotitanium alloy and manufacturing titanium dioxide. According to usgs2021 statistics, the world's titanium ore resources are about 740 million tons (by TiO_2 content), of which more than 90 pct are titanium and iron symbiotic ore.[18] The titanium magnetite ore as important iron ore has been successfully used in the BF iron making process. However, the reduction of TiO_2 will make the smelting abnormal. Therefore, some blast furnace plants use a blend of titano-magnetite ore with the normal iron ore to control the TiO_2 content (less than 23 wt pct) in the slag.[19,20] HIsarna has the potential to smelt this type of ore with one-hundred percent feed, which will potentially open up a vast new paradigm for iron ore. Therefore, the titanium magnetite ore injection into HIsarna practice has been calculated *via* the developed model. The productivity and kinetic parameters are kept the same during the calculation. The composition of the injected titanium magnetite ore is shown in Table III. Compared with the iron concentrate in Table II, besides the higher TiO_2 content, the injected titanium magnetite ore also has higher FeO, Al_2O_3, and MgO contents. The LOI is considered as carbonate decomposition.

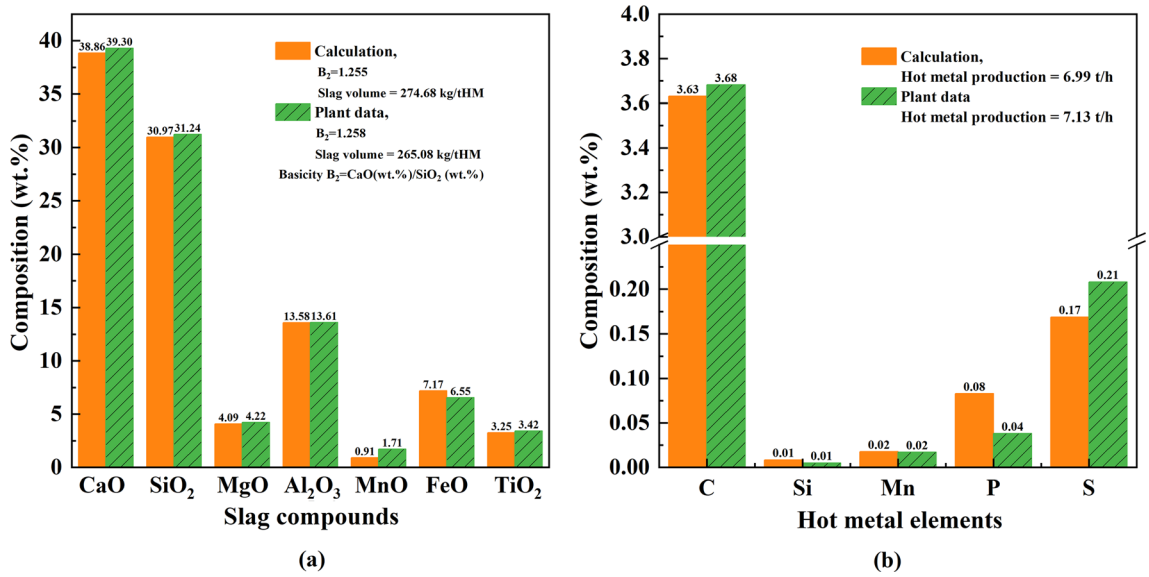

Fig. 3—Comparison of the calculated compositions of (*a*) slag and (*b*) hot metal with pilot plant data.

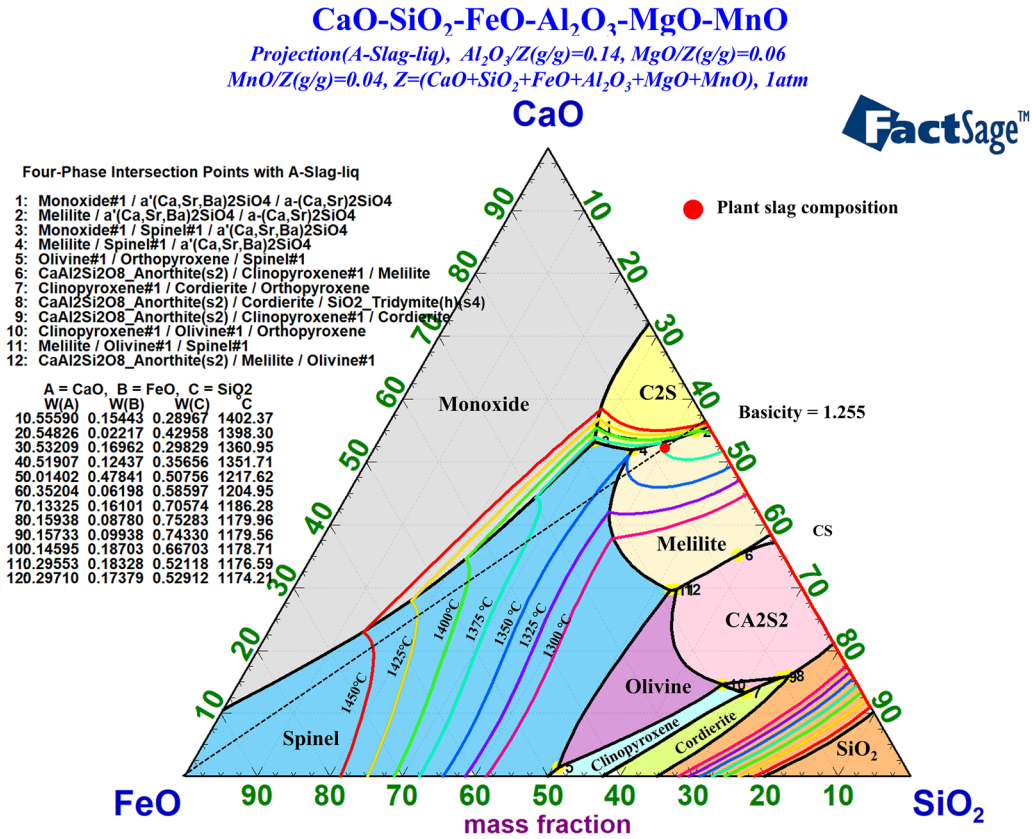

Fig. 4—Liquidus projection of CaO-SiO_2-MgO-Al_2O_3-FeO slag system.

The model input and output before and after titanium magnetite ore injection are shown in Figure 6. To ensure the same productivity, the amount of injected titanium magnetite ore with lower iron grade has been increased, as well as the dust. The lime consumption is decreased because the basicity of the slag is decreased since high TiO_2 slag cannot maintain high basicity at the operating temperature, which will be discussed in detail later. Coal consumption also shows a slight decrease, mainly due to the high FeO content in the titanium magnetite ore

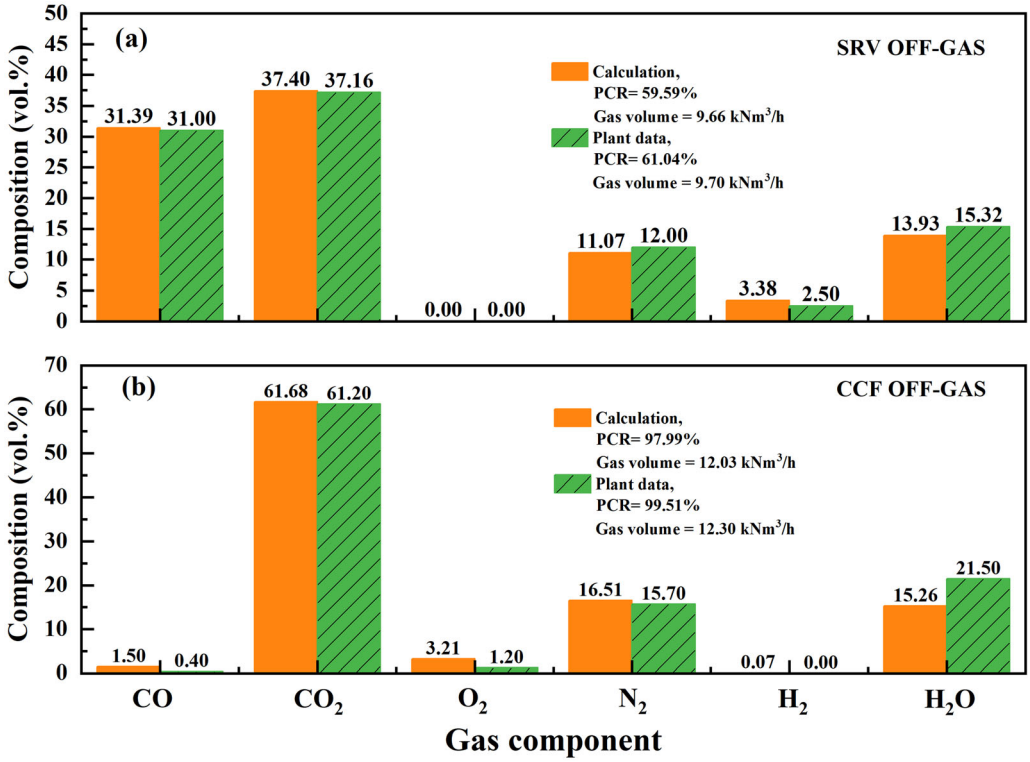

Fig. 5—Comparison of the calculated compositions of SRV gas (*a*), and CCF gas (*b*) with pilot plant data.

Table III. Composition of Titanium Magnetite Ore (Wt PCt)

	Fe_2O_3	FeO	Al_2O_3	SiO_2	CaO	MgO	MnO	TiO_2	P_2O_5	S	Moisture	LOI	Total
Titanium Magnetite Ore	52.19	27.93	3.65	2.99	1.15	3.00	0.72	7.35	0.09	0.015	0.21	0.70	100

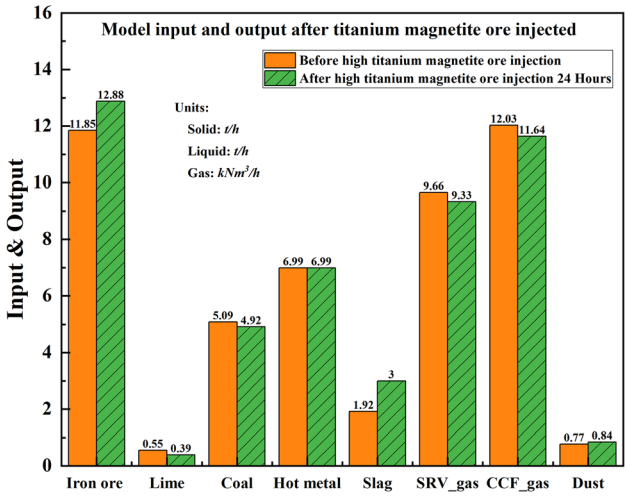

Fig. 6—Model input and output before and after titanium magnetite ore injection.

which reduces part of the carbon consumption used to reduce Fe_2O_3 to FeO. Correspondingly, due to the reduced use of coal, off-gas (SRV & CCF) volume also decreased. The higher gangue content in titanium magnetite ore resulted in an increase in the slag volume.

The composition change of slag, hot metal, and off-gas during the titanium magnetite ore injection is shown in Figure 7. After 24 h of injection of titanium magnetite ore, the composition of the slag and the molten iron tend to be stable. The slag basicity decreases from 1.25 to 1.11. The TiO_2 content in slag is close to 25 wt pct when fully using this kind of ore. As expected, the MgO and Al_2O_3 content also increased in the slag due to the high MgO and Al_2O_3 content of the titanium magnetite ore. No significant change is observed in FeO and MnO content in slag. The composition of hot metal is shown in Figure 7(b). The carbon content decreases from 3.6 to about 3.3 due to the decrease in coal injection when keeping the same kinetic parameters, decreasing carbon used for carburizing. Because of the decline of phosphorus load and the increase of sulfur load (mainly caused by the difference in phosphorus and sulfur content in iron ore), phosphorus and sulfur contents in the hot metal also changed accordingly. The off-gas composition of SRV and CCF is shown in Figures 7(c) and (d). As the injected coal was reduced, the CO_2 in the off-gas gases increased. There are about 2.5 vol pct of H_2 and 25 vol pct of CO remaining in the SRV off-gas and almost all are combusted in CCF. The PCR increased in both SRV and CCF.

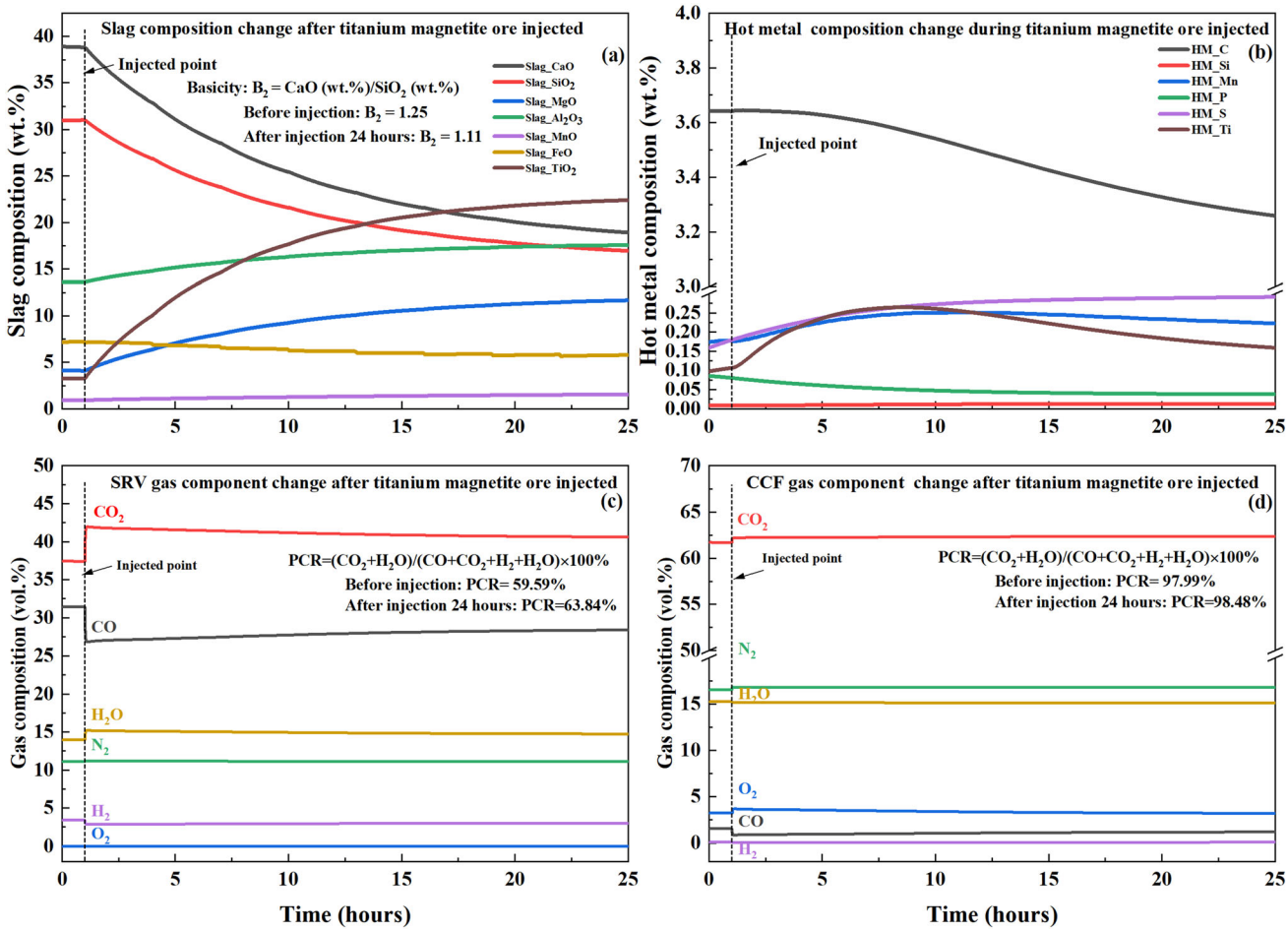

Fig. 7—The composition changes during the titanium magnetite ore injection: (*a*) slag, (*b*) hot metal, (*c*) SRV off-gas, and (*d*) CCF off-gas.

The slag properties play a significant role in the pyrometallurgical processes. In particular, for titania-containing slag, there have been reports of abnormalities in blast furnace operation, such as high viscosity, low sulfide capacity, and slag foaming.[20–24] It is necessary to study and optimize the high titania slag in the HIsarna process using titanium magnetite ore. The phase diagram and liquids of TiO_2-CaO-SiO_2-(17 wt pct)Al_2O_3-(11 wt pct)MgO-(6 wt pct)FeO slag system are shown in Figure 8. The red point is the slag composition when using titanium magnetite ore, and the dotted line presents the basicity at 1.10. The slag liquidus is lower than 1475 °C, but still higher than 1450°C (HIsarna practice temperature) even though the basicity decreased to 1.10. The first precipitated phase is titania spinel (magnesia alumina spinel containing titania). Obviously, increasing the operating temperature will increase coal consumption and accelerate the corrosion of refractory materials in the hearth. In order to lower the liquidus of the slag, it is necessary to control the magnesia and alumina contents in the slag. According to the author's previous work,[25] the liquidus of CaO-SiO_2-8wt pct MgO-14wt pct Al_2O_3- *x* wt pctTiO_2 (basicity = 1.10, *x* from 0 to 40 wt pct) slag system is less than 1425 °C, and the viscosity decreases with increasing TiO_2 content in neutral or inert atmosphere. In the BF process, the TiO_2 in slag is reduced to Ti(C, N) in the strong reducing atmosphere, which is the main reason for the poor fluidity and foaming of the slag.[19] These high-melting solid phases increase the slag viscosity and strengthen the stability of the bubbles in the slag. The HIsarna slag has a higher oxygen potential, and TiO_2 will not be reduced to Ti(C, N), but the injected coal may become a new solid phase source. Although the physical and chemical properties of titania-containing slag have been well documented,[26] the titanium slag system suitable for the HIsarna process still needs more investigation.

C. *Heat Profiles*

The thermal efficiency and heat distribution of the reactor are critical to energy utilization. The calculated heat distribution and heat load of the HIsarna process before and after titanium magnetite ore injection have been shown in Figure 9. The most significant heat consumption is in reactions (*e.g.*, reduction of iron ore, coal pyrolysis, and gasification), followed by off-gas sensible heat and heat loss. It shows a high proportion of the input energy consumed in the sensible heat of off-gas, approximately one-third of the total heat. In the HIsarna process, the off-gas from the SRV is

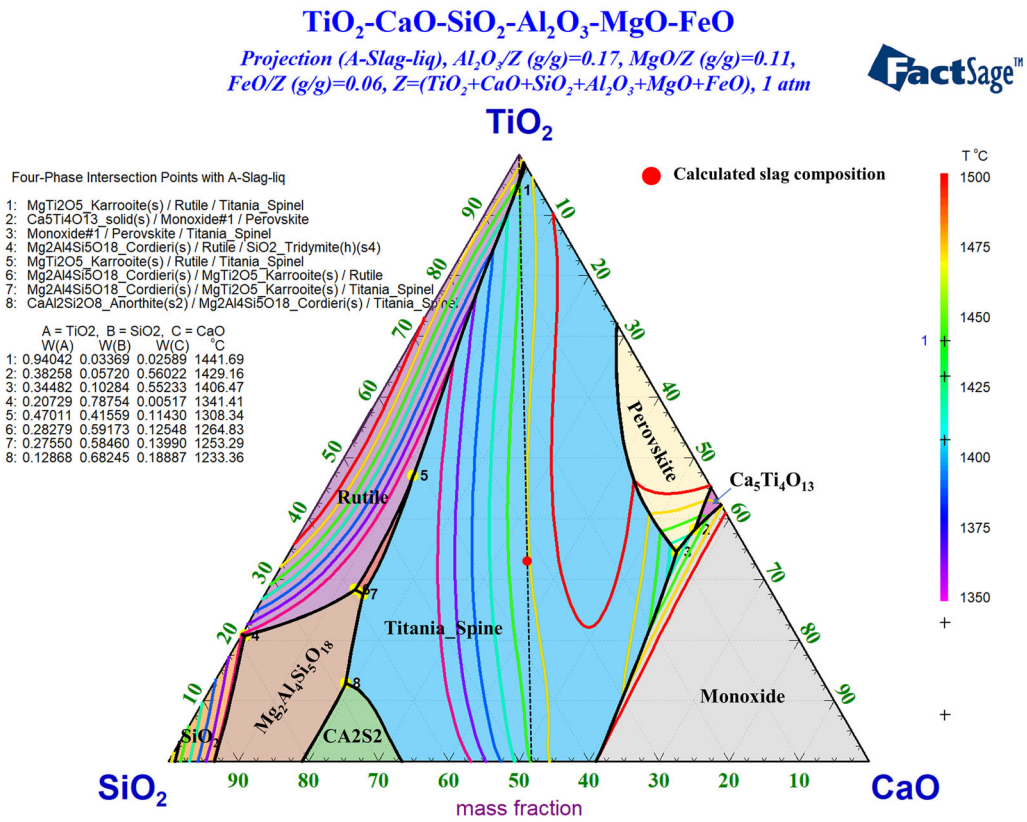

Fig. 8—Liquidus projection of TiO_2-CaO-SiO_2 -Al_2O_3-MgO-FeO slag system.

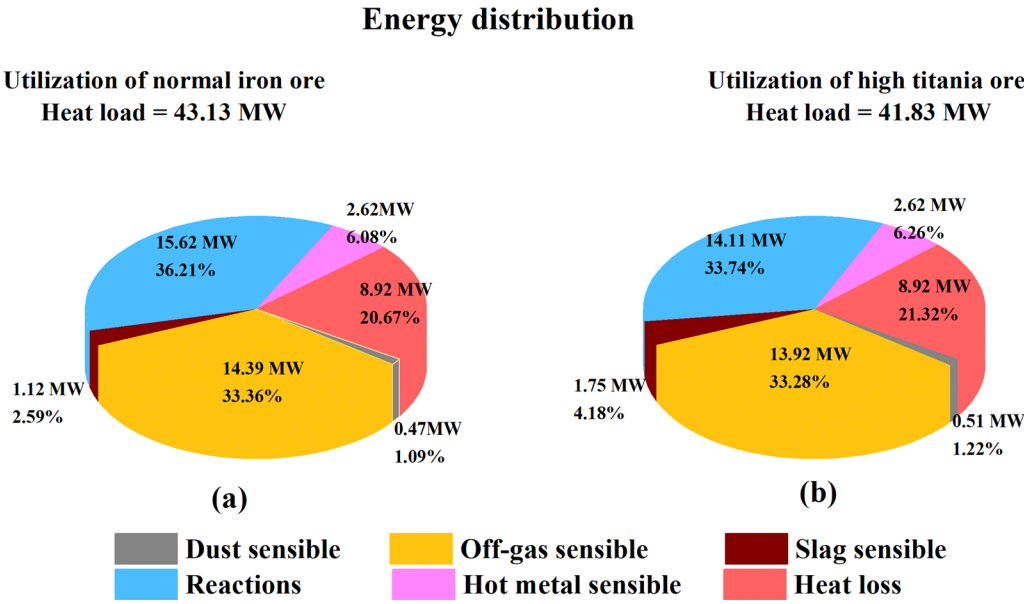

Fig. 9—The calculated heat distribution of utilization of normal iron ore (*a*) and high titania ore (*b*).

post-combusted in the CCF, which creates the high temperature for iron ore pre-reduction and melting. The temperature of CCF off-gas reflects the heat transfer efficiency of the cyclone and, ideally, it should be close to the melting temperature of the pre-reduced iron ore, which is approximately 1400 °C. While from the pilot plant data, the temperature of the off-gas is higher than this value due to heat transfer limitations. In this case, the CCF off-gas with a high temperature is inevitable, but this high-grade heat can be recovered efficiently in a

waste heat recovery unit. The heat loss accounts for about 20 pct of the input energy and mainly comes from the water cooling panels of the SRV, cyclone, and off-gas duct. The specific surface area of the furnace (the ratio of the surface area and the volume of the furnace) decreases with increasing of furnace volume: area scales with the diameter to the second power, while volume scales to the third power. Therefore, the heat losses to cooling water are larger on a pilot scale than in an industrial plant. In addition, the increase in productivity further lowers the specific losses to the water cooling. An up-scaled plant calculation based on similar consumptions and a nominal annual production of 1 million tons shows that the heat loss falls significantly to about 11 pct of the input energy.[27] Compared with the energy distribution of utilization of typical iron ore, the heat load decreases after the titanium magnetite ore injection due to the decrease in coal consumption. The energy needed for the reactions decreases mainly due to the high FeO content in magnetite ore. The increased slag volume responds to the increase of slag sensible heat.

IV. SUMMARY

Based on the effective equilibrium reaction zone model (EERZ) concept, a kinetic HIsarna process simulation model has been developed using the FactSage macro processing facility. Twelve reaction zones, including combustion, coal pyrolysis and gasification, slag/carbon reaction, and slag/metal reaction, were considered in the proposed model. The model has also been used to investigate the utilization of titanium magnetite ore in the process. In conclusion, the model can accurately predict the slag, hot metal, SRV gas, and CCF gas composition with respect to pilot plant data. The HIsarna process shows promising potential in using low-quality/difficult-to-use iron ore as feed materials, such as titanium magnetite ore, but further investigation is needed as the slag system needs to be optimized. The off-gas sensible heat accounts for a large part of the input heat due to the high temperature, which can be recovered efficiently. Titanium magnetite ore injection decreases the coal consumption and the heat load.

ACKNOWLEDGMENTS

The authors are pleased to acknowledge the financial support from EPSRC under the grant number EP/N011368/1 (EPSRC Fellowship). The authors also want to thank the IJmuiden Technology Centre of Tata Steel Europe for sharing vast amounts of their pilot plant data to develop this model.

CONFLICT OF INTEREST

On behalf of all authors, the corresponding author states that there is no conflict of interest.

OPEN ACCESS

REFERENCES

1. W.S. Association: "Steel's contribution to a low carbon future and climate resilient societies" https://www.apeal.org/wp-content/uploads/2015/03/Steel_s-contribution-to-a-low-carbon-future.pdf.pdf.
2. J. van Boggelen, H. Meijer, C. Zeilstra, H. Hage and P. Broersen: *Proc. 2019 Eurocoke Summit, April 3–4* (2019).
3. D. Khasraw, Z. Yan, J.L. Hage, K. Meijer, and Z. Li: *Metall. Mater. Trans. B.*, 2022, vol. 53B, pp. 3246–61.
4. T.T. Htet, Z. Yan, D. Khasraw, J. Hage, and K. Meijer: *Z. Li*, 2022, https://doi.org/10.1007/s11663-022-02677-1.
5. B. Srivastava, S. Roy, and P. Sen: *Metall. Mater. Trans. B.*, 2010, vol. 41B, pp. 935–39.
6. A. Kadrolkar, S.K. Roy, and P.K. Sen: *Metall. Mater. Trans. B.*, 2012, vol. 43B, pp. 173–85.
7. C. Srishilan and A.K. Shukla: *Metall. Mater. Trans. B.*, 2019, vol. 50B, pp. 312–23.
8. B. Kumar, S. Mishra, G.G. Roy, and P.K. Sen: *Steel Res. Int.*, 2017, vol. 88, pp. 339–42.
9. M.A. Van Ende, Y.M. Kim, M.K. Cho, J. Choi, and I.H. Jung: *Metall. Mater. Trans. B.*, 2011, vol. 42B, pp. 477–89.
10. M.A. Van Ende and I.H. Jung: *Metall. Mater. Trans. B*, 2017, vol. 48B, pp. 28–36.
11. M.A. Van Ende and I.H. Jung: *ISIJ Int.*, 2014, vol. 42, pp. 489–95.
12. D. Thompson and B. Argent: *Miner. Process. Extr Metall.*, 2007, vol. 116, pp. 115–22.
13. E. Moosavi-Khoonsari, M.A. Van Ende, and I.H. Jung: *Metall. Mater. Trans. B.*, 2022, vol. 53B, pp. 981–98.
14. D. Kumar, K.C. Ahlborg, and P.C. Pistorius: *Metall. Mater. Trans. B.*, 2019, vol. 50B, pp. 2163–74.
15. FactSage, Date Access Year 2022. www.factsage.com.
16. C. Bale, E. Bélisle, P. Chartrand, S. Decterov, G. Eriksson, K. Hack, I.-H. Jung, Y.-B. Kang, J. Melançon, and A. Pelton: *Calphad*, 2009, vol. 33, pp. 295–311.
17. K. Meijer, C. Guenther and R. Dry: *In Proc. 1st Int. Conf. on Energy Efficiency and CO_2 Reduction in the Steel Industry*, 2011. Access: http://dl.iran-mavad.com/sell/trans/en/HIsarna/Pilot/Plant/Project.pdf.
18. "Mineral Commodity Summaries 2021" (https://pubs.er.usgs.gov/publication/mcs2021, Date Access Year 2021.
19. Z. Pang, X. Lv, J. Ling, Y. Jiang, Z. Yan, and J. Dang: *Metall. Mater. Trans. B.*, 2020, vol. 51B, pp. 2348–57.
20. Z. Pang, X. Lv, Y. Jiang, J. Ling, and Z. Yan: *Metall. Mater. Trans. B.*, 2020, vol. 51B, pp. 722–31.
21. Z. Pang, Y. Jiang, J. Ling, X. Lv and Z. Yan, *Int. J. Miner., Metall. Mater.*, 2022, vol. 29, pp. 1170–78.
22. J. Ling, Z. Pang, Y. Jiang, Z. Yan, and X. Lv: *Metall. Mater. Trans. B.*, 2021, vol. 52B, pp. 2786–95.

23. J. Xiang, X. Wang, M. Yang, J. Wang, C. Shan, G. Fan, G. Qiu, and X. Lv: *J. Mater. Res. Technol.*, 2021, vol. 34, pp. 629–41.
24. J. Xiang, J. Wang, Q. Li, C. Shan, G. Qiu, W. Yu, and X. Lv: *Can. Metall. Q.*, 2020, vol. 59, pp. 151–58.
25. X. Lv. Z. Yan, W. He, J., *ISIJ Int.,* 2017, vol. 57, pp. 31–36.
26. Z. Yan, X. Lv, and Z. Li: *J Iron Steel Res Int.*, 2021, vol. 29, pp. 187–206.
27. C. Grisvard, J. Lövgren, J. Boggelen, et al.: *European Commission, Directorate-General for Research and Innovation*: Hisarna experimental campaigns B and C (HIsarna B and C), Publications Office, 2015. https://data.europa.eu/doi/10.2777/107258.